Parametric Design of Open Ended Waveguide Array Feeder with Reflector Antenna for Switchable Cosecant-Squared Pattern

Okan Mert Yucedag [1,2], Ahmet Serdar Turk [1]

[1] Yildiz Technical University, Electronics and Telecommunication Engineering Department
Esenler, 34220, Istanbul, TURKEY
asturk@yildiz.edu.tr

[2] TUBITAK Center of Research for Advanced Technologies of Informatics and Information Security
P.O. Box 21, Gebze, 41470, Kocaeli, TURKEY
okanmert.yucedag@bte.tubitak.gov.tr

Abstract **─** This paper presents parametric analysis of two-dimensional (2D) open-ended waveguide array feeder and introduces a modified parabolic reflector antenna structure to obtain electronically switchable radiation patterns. The main motivation of the study is to achieve desired radiation characteristics for naval, air and coastal surveillance radars such as, pencil beam, suppressed side lobes and cosecant-squared pattern shapes. The Analytical Regularization Method (ARM) is used as a fast and accurate pre-design tool to compute near and far field radiation characteristics of the feeder and reflector antennas. The numerical procedure is initially verified by the analytical methods and the calculated results are presented for the proposed novel designs.

Index Terms **─** Open-ended waveguide array, Parabolic reflector antenna, Cosecant squared pattern, Analytical regularization method.

I. INTRODUCTION

Typical surveillance radar systems generally have a parabolic reflector, which has cosecant-squared elevation pattern [1]. The feeder configurations must be considered primarily to estimate the radiation characteristics of reflector conveniently. Waveguide or horn antenna arrays are widely used to feed the reflector antennas. Suitable feeder configurations, which can illuminate the reflector efficiently, must be designed to meet requirements of modern radar systems. Geometrical optics (GO), physical optics (PO), aperture integration (AI) and geometric theory of diffraction (GTD), or optimization methods can be used for determining the antenna radiation characteristics [2-6]. Moreover, method of moments (MoM), finite element method (FEM) and finite difference methods can be used for feeder and reflector designs [7-8]. However, large size antenna analyses usually require long computation times [9-10]. Furthermore, the complexity of some cavity or aperture geometries creates hard numerical convergence problems in many cases. The origin of these problems is related to the direct numerical methods, which reduce a diffraction boundary value problem (BVP) to the functional equation of the first kind. First kind equations may typically have a singular kernel that causes unstable numerical process. Thus, while the truncation number of the matrix-vector algebraic equation set increases, computational error degradation cannot be guaranteed [11-13]. Hence, ARM that transforms the ill-conditioned integral equation of the first kind into a well-conditioned one of the second

Submitted On: April 23, 2012
Accepted On: July 22, 2012

1054-4887

kind is preferred to solve the matrix equation numerically by truncation method with fast convergence to reach fast and reliable solutions [14]. The ARM is implemented for solving the 2D problem of E-polarized wave diffraction by arbitrary shaped, smooth and perfectly conductive cylindrical obstacles to obtain fast, accurate and reliable results [15-16]. The ARM solutions for the 2D parabolic reflector and the H-plane horn feeder have already been demonstrated by Turk [10, 18-20].

In this paper, parametric characterization of the 2D open-ended waveguide array feeder and the design of modified reflector antenna are presented to achieve electronically switchable pencil beam and cosecant-squared radiation patterns for naval, air and coastal surveillance radars. Feeder is located on the focus of the reflector. Geometry of the problem is illustrated in Fig. 1.

Section II explains the general theory of ARM. Section III presents the parametric analysis of wave guide array feeder. Section IV describes the reflector design for pencil-beam and cosecant-squared switchable pattern with exhibition of performance results. Section V is the conclusion.

II. ARM FORMULATION

Scalar diffraction problem of an infinitely long, smooth, longitudinally homogeneous and perfectly conducting cylindrical obstacle corresponds to the Dirichlet boundary condition for E-polarized incident wave. The incident and scattered scalar wave functions ($u^i(p)$ and $u^s(p)$) must satisfy the Helmholtz equation given in Eq. (1) and the Dirichlet boundary condition in (2), also with the Sommerfeld radiation condition.

$$\left(\Delta + k^2\right)u^s(p) = 0, \quad p \in R^2 \backslash S \tag{1}$$

$$u^{s(+)}(p) = u^{s(-)}(p) = -u^i(p), \quad p \in S \tag{2}$$

where, S is smooth XOY cross section contour of the domain D in 2D space $R^2 \in C^2$, $u^{s(+)}(p)$ and $u^{s(-)}(p)$ are limiting values of $u^s(p)$ in the inner and the outer sides of S, respectively. The solution of the BVP is written in (3), using the Green's formula and the boundary condition in (2) [14].

$$-\frac{i}{4}\int_S \left[H_0^{(1)}(k\,|\,q-p\,|)Z(p)\right]dl_p = -u^i(q) \tag{3}$$

where, $Z(p) = \dfrac{\partial u^{s(-)}(p)}{\partial n} - \dfrac{\partial u^{s(+)}(p)}{\partial n}, \quad q, p \in S$; n is the unit outward with respect to S normal of the point p. The unknown function $Z(p)$ is constructed by solving (3), and using parameterization of the S contour specified by the function $\eta(\theta)=(x(\theta),y(\theta))$ that smoothly parameterizes the S by $\theta\in[-\pi,\pi]$. The integral equation representation of the first kind in (3) is equivalently arranged as follows:

$$\frac{1}{2\pi}\int_{-\pi}^{\pi}\left[\ln\left|2\sin\frac{\theta-\tau}{2}\right| + K(\theta,\tau)\right]Z_D(\tau)d\tau = g(\theta) \tag{4}$$

with the unknown function $Z_D(\tau)$ and the given function $g(\theta)$, where $\theta \in [-\pi,\pi]$ and

$$Z_D(\theta) = l(\theta)Z(\eta(\theta)), g(\theta) = -u^i(\eta(\theta)) \tag{5}$$

$$l(\theta) = \sqrt{[x'(\theta)]^2 + [y'(\theta)]^2} > 0, \quad x(\theta), y(\theta) \in C^\infty\left(Q^1\right) \tag{6}$$

The logarithmic part in (4) represents the main singularity and $K(\theta,\tau)$ is rather smooth section of the Green's function. The functions in (4) are represented by their Fourier series expansions with $k_{s,m}$, z_m, g_m coefficients. An infinite system of the linear algebraic equations of the second kind can be obtained [15]:

$$\hat{z}_s + \sum_{m=-\infty}^{\infty}\hat{k}_{s,m}\hat{z}_m = \hat{g}_s, \quad s = \pm 1, \pm 2, .. \tag{7}$$

where

$$\begin{aligned} \hat{k}_{s,m} &= -2\tau_s\tau_m\left[k_{s,-m} + \frac{1}{2}\delta_{s,0}\delta_{m,0}\right], \\ \hat{z}_n &= \tau_n^{-1}z_n,\ \hat{g} = -2\tau_s g_s \\ \tau_n &= \max(1, |\,n\,|^{1/2}), \quad n = 0, \pm 1, \pm 2, .. \end{aligned} \tag{8}$$

and $\delta_{s,0}$ is the Kronecker delta function. Finally, the scattered field $u^s(q)$ for $q \in R^2$ is obtained by the integral equation representation of the (4) with any required accuracy by the truncation method [16].

The ARM procedure has already been verified by the analytical solution of wave scattering from infinitely long circular cylinder [10]. Moreover, it is compared with the analytical Wiener-Hopf solution of scattering from parallel-plate waveguide cavity for the case of E-polarized plane wave incidence from 60°, which is given in Fig. 2 [17].

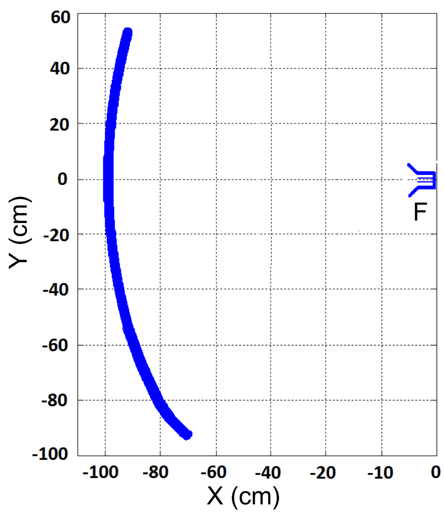

Fig. 1. XOY-plane geometry of reflector antenna.

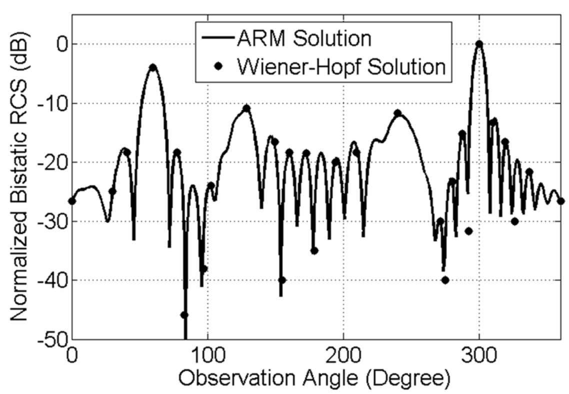

Fig. 2. Comparison of the ARM calculation with analytical result of scattering from open-ended waveguide for 60° plane wave incidence.

III. PARAMETRIC ANALYSIS OF WAVEGUIDE ARRAY FEEDER

The ARM procedure described at Section II is derived for the investigated waveguide array feeder. The geometrical cross-section of the feeder is modeled by ARM, as a closed contour L that goes from point A to point Z and back to A corresponding to $\theta\in[-\pi,\pi]$, as illustrated in Fig. 3. The relation between l and θ is formulated in (9). Distances of sources from inner wall are $\lambda/4$.

$$\left.\begin{array}{l} l=(\theta+\pi)L/2\pi \\ l\in[0,L]\rightarrow(\theta,\tau)\in[-\pi,\pi] \end{array}\right\} \quad (9)$$

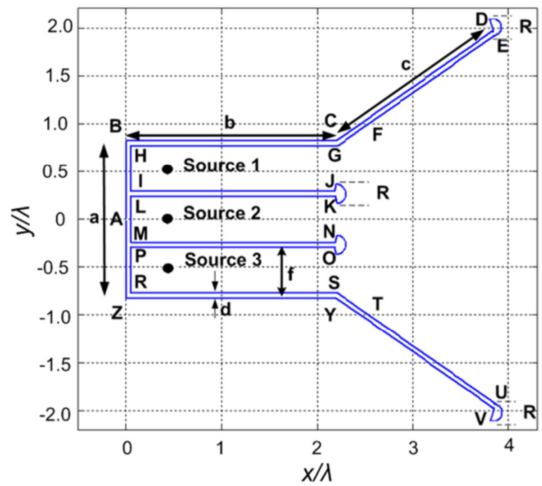

Fig. 3. XOY-plane geometry of 3-elements open-ended and flared waveguide array.

The feeder structure consists of totally 23 contour parts that are defined in Table I. The parameterization of the contour line is implemented separately from point A to Z, and back to A by means of the variable $l\in[0,L]$ as given in Table 1 and Table 2.

Parametric analysis results of the waveguide length, waveguide width, flare angle and edge rolling effects on the H-plane radiation pattern are presented in Figs. 4-7, respectively. The major comments are highlighted briefly that; increasing the waveguide length decreases back lobe levels (see Fig. 4). The waveguide width should be arranged as less than 0.75λ to avoid multi-mode propagation (see Fig. 5). Increasing the flare angle does not yield significant effect for waveguide array (see Fig. 6), although it can suppress back lobe levels up to 15 dB for the single horn [20]. The edge rolling can slightly improve the side and back lobe suppression performance (see Fig. 7).

Since electronically shaping of the reflector radiation pattern mainly depends on the aperture illumination, the most critical design parameter of the feeder is source phases. The electronically beam scanning performance of the waveguide array feeder is demonstrated in Fig. 8. The phase difference of 7° is proposed to obtain the near field illumination in Fig. 11 for the suitable cosecant-squared pattern given in Fig. 12.

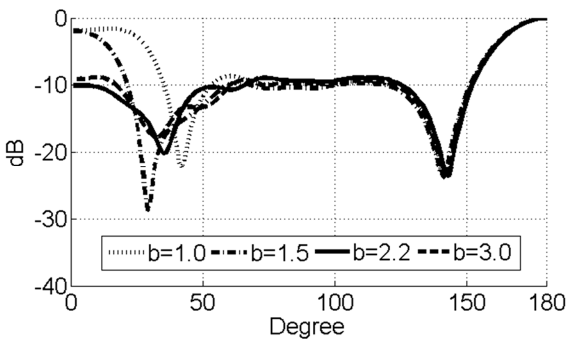

Fig. 4. H-plane radiation pattern of the feeder for *c=2λ, d=0.05λ, f=0.481λ, R=1λ, α =25°.*

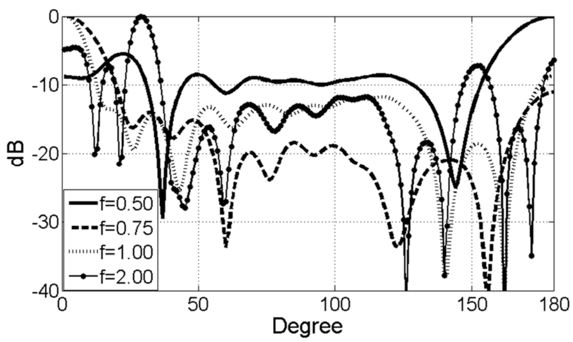

Fig. 5. H-plane radiation pattern of the feeder for *b=2.2λ, c=2.0λ d=0.05λ, R=1λ, α =25°.*

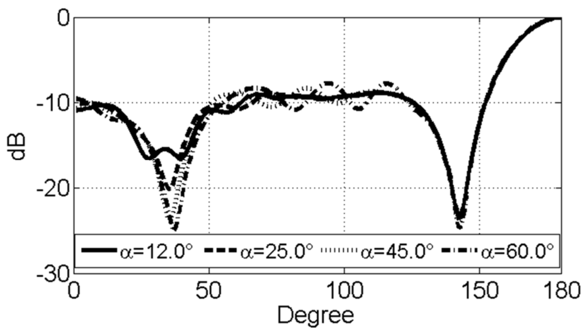

Fig. 6. H-plane radiation pattern of the feeder for *b=2.2λ, c=2λ, d=0.05λ, f=0.481λ, R=1λ.*

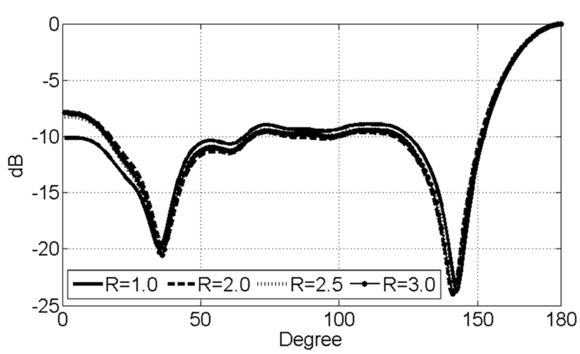

Fig. 7. H-plane radiation pattern of the feeder for *b=2.2λ, c=2.0λ, d=0.05λ, f=0.481λ, α =25°.*

Table 1: Segment lengths of the feeder contour regions

No	Segment Definition	Segment Length
1	$-\pi \le \theta < 2L_1\frac{\pi}{L}-\pi$	$L_1 = a$
2	$2L_1\frac{\pi}{L}-\pi \le \theta < 2L_2\frac{\pi}{L}-\pi$	$L_2 = L_1 + b$
3	$2L_2\frac{\pi}{L}-\pi \le \theta < 2L_3\frac{\pi}{L}-\pi$	$L_3 = L_2 + c$
4	$2L_3\frac{\pi}{L}-\pi \le \theta < 2L_4\frac{\pi}{L}-\pi$	$L_4 = L_3 + 0.5\pi Rd$
5	$2L_4\frac{\pi}{L}-\pi \le \theta < 2L_5\frac{\pi}{L}-\pi$	$L_5 = L_4 + c - d/\tan\alpha_1$
6	$2L_5\frac{\pi}{L}-\pi \le \theta < 2L_6\frac{\pi}{L}-\pi$	$L_6 = L_5 + d/\sin\varphi_1$
7	$2L_6\frac{\pi}{L}-\pi \le \theta < 2L_7\frac{\pi}{L}-\pi$	$L_7 = L_6 + b - db_1 + d$
8	$2L_7\frac{\pi}{L}-\pi \le \theta < 2L_8\frac{\pi}{L}-\pi$	$L_8 = L_7 + f$
9	$2L_8\frac{\pi}{L}-\pi \le \theta < 2L_9\frac{\pi}{L}-\pi$	$L_9 = L_8 + b - d$
10	$2L_9\frac{\pi}{L}-\pi \le \theta < 2L_{10}\frac{\pi}{L}-\pi$	$L_{10} = L_9 + 0.5\pi Rd$
11	$2L_{10}\frac{\pi}{L}-\pi \le \theta < 2L_{11}\frac{\pi}{L}-\pi$	$L_{11} = L_{10} - d + b$
12	$2L_{11}\frac{\pi}{L}-\pi \le \theta < 2L_{12}\frac{\pi}{L}-\pi$	$L_{12} = L_{11} + f$
13	$2L_{12}\frac{\pi}{L}-\pi \le \theta < 2L_{13}\frac{\pi}{L}-\pi$	$L_{13} = L_{12} + b - d$
14	$2L_{13}\frac{\pi}{L}-\pi \le \theta < 2L_{14}\frac{\pi}{L}-\pi$	$L_{14} = L_{13} + 0.5\pi Rd$
15	$2L_{14}\frac{\pi}{L}-\pi \le \theta < 2L_{15}\frac{\pi}{L}-\pi$	$L_{15} = L_{14} - d + b$
16	$2L_{15}\frac{\pi}{L}-\pi \le \theta < 2L_{16}\frac{\pi}{L}-\pi$	$L_{16} = L_{15} + f$
17	$2L_{16}\frac{\pi}{L}-\pi \le \theta < 2L_{17}\frac{\pi}{L}-\pi$	$L_{17} = L_{16} + b - db_2 + d$
18	$2L_{17}\frac{\pi}{L}-\pi \le \theta < 2L_{18}\frac{\pi}{L}-\pi$	$L_{18} = L_{17} + d/\sin\varphi_2$
19	$2L_{18}\frac{\pi}{L}-\pi \le \theta < 2L_{19}\frac{\pi}{L}-\pi$	$L_{19} = L_{18} + c - d/\tan\alpha_2$
20	$2L_{19}\frac{\pi}{L}-\pi \le \theta < 2L_{20}\frac{\pi}{L}-\pi$	$L_{20} = L_{19} + 0.5\pi Rd$
21	$2L_{20}\frac{\pi}{L}-\pi \le \theta < 2L_{21}\frac{\pi}{L}-\pi$	$L_{21} = L_{20} + c$
22	$2L_{21}\frac{\pi}{L}-\pi \le \theta < 2L_{22}\frac{\pi}{L}-\pi$	$L_{22} = L_{21} + b$
23	$2L_{22}\frac{\pi}{L}-\pi \le \theta < 2L_{23}\frac{\pi}{L}-\pi$	$L = L_{22} + a$
$db_1 = d/\tan\varphi_1 - d/\tan\alpha_1 - 0.5d\sin\alpha_1$ $db_2 = d/\tan\varphi_2 - d/\tan\alpha_2 - 0.5d\sin\alpha_2$		

Table 2: Parametric definitions of feeder contour

No	Region	Parameterization
1	*AB*	$x=0\ ;\ y=l-L_1+a$
2	*BC*	$x=l-L_1\ ;\ y=a$
3	*CD*	$x=b+(l-L_2)\cos(\alpha_1);\ y=a+(l-L_2)\sin(\alpha_1)$
4	*DE*	$x=0.5d\sin(\alpha_1)+b+c\cos(\alpha_1)+0.5Rd\cos(0.5\pi+\alpha_1)$ $-2(l-L_3)/Rd+X_0;$ $y=-0.5d\cos(\alpha_1)+a+c\sin(\alpha_1)+0.5Rd\sin(0.5\pi+\alpha_1)$ $-2(l-L_3)/Rd+Y_0;$ $X_0=0.5(1-R)d\sin(\alpha_1);Y_0=0.5(R-1)d\cos(\alpha_1)$
5	*EF*	$x=b+d\sin(\alpha_1)+(c-(l-L_4))\cos(\alpha_1);$ $y=a-d\cos(\alpha_1)+(c-(l-L_4))\sin(\alpha_1);$
6	*FG*	$x=d/\sin(\alpha_1)+b-(l-L_5)\cos(\varphi_1);$ $y=a-(l-L_5)\sin(\varphi_1);$
7	*GH*	$x=-l+L_6+b-db1;\ y=a-d;$
8	*HI*	$x=d;\ y=-l+L_7+a-d;$
9	*IJ*	$x=l-L_8+d;\ y=a-d-f;$
10	*JK*	$x=b+0.5R_1d\cos(\pi/2-2(l-L_9)/(R_1d));$ $y=a-1.5d-f+0.5R_1d\sin(\pi/2-2(l-L_9)/(R_1d));$
11	*KL*	$x=L_{10}-l+b;\ y=a-2d-f;$
12	*LM*	$x=d;\ y=L_{11}-l+a-2d-f;$
13	*MN*	$x=l-L_{12}+d;\ y=a-2d-2f;$
14	*NO*	$x=b+0.5R_1d\cos(\pi/2-2(l-L_{13})/(R_1d));$ $y=a-2.5d-2f+0.5R_1d\sin(\pi/2-2(l-L_{13})/(R_1d));$
15	*OP*	$x=L_{14}-l+b;\ y=a-3d-2f;$
16	*PR*	$x=d;\ y=L_{15}-l+a-3d-2f;$
17	*RS*	$x=l-L_{16}+d;\ y=d-a;$
18	*ST*	$x=b-db2+(l-L_{17})\cos(\varphi_2);$ $y=d-a-(l-L_{17})\sin(\varphi_2)$
19	*TU*	$x=b+d/\tan(\alpha_2)-db2+(l-L_{18})\cos(\alpha_2);$ $y=-a-(l-L_{18})\sin(\alpha_2)$
20	*UV*	$x=0.5d\sin(\alpha_2)+b+c\cos(\alpha_2)+0.5Rd\cos(0.5\pi-\alpha_2)$ $-2(l-L_{19})/Rd+X_0;$ $y=-0.5d\cos(\alpha_2)+a+c\sin(\alpha_2)+0.5Rd\sin(0.5\pi-\alpha_2)$ $-2(l-L_{19})/Rd+Y_0;$ $X_0=0.5(R-1)d\sin(\alpha_2);Y_0=0.5(R-1)d\cos(\alpha_2)$
21	*VY*	$x=0.5d\sin(\alpha_2)+b+c\cos(\alpha_2)+0.5Rd\cos(0.5\pi-\alpha_2)$ $-2(l-L_{19})/Rd+X_0;$ $y=-0.5d\cos(\alpha_2)+a+c\sin(\alpha_2)+0.5Rd\sin(0.5\pi-\alpha_2)$ $-2(l-L_{19})/Rd+Y_0;$ $X_0=0.5(R-1)d\sin(\alpha_2);Y_0=0.5(R-1)d\cos(\alpha_2)$
22	*YZ*	$x=b+L_{21}-l;\ y=-a;$
23	*ZA*	$x=0;\ y=-a+l-L_{22};$

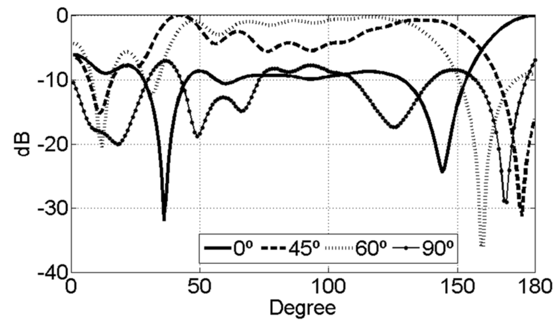

Fig. 8. Electronically scanned H-plane radiation pattern of the feeder for *b=2.2λ, c=2λ, d=0.05λ, f=0.5λ, R=1λ, α =30°.*

IV. REFLECTOR DESIGN WITH ELECTRONICALLY SWITCHABLE PATTERN

The geometrical cross-section of the reflector is modeled by ARM, as a closed contour *L* that starts from point *A* towards point *M* and returns to *A* corresponding to $\theta\in[-\pi,\pi]$, as illustrated in Fig. 9. The relation between l and θ is formulated in (9).

The reflector structure consists of totally 12 contour parts. The parameterization of the contour line is implemented separately from point *A* to *M,* and back to *A* by means of the variable $l\in[0,L]$ as given in Table 3 and Table 4.

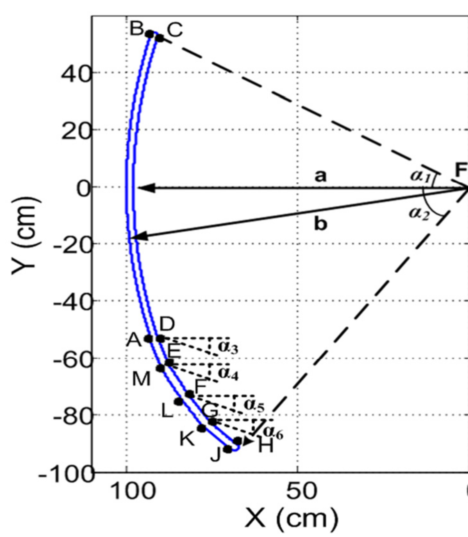

Fig. 9. Geometry of the modified reflector.

The modified reflector geometry is designed asymmetrically by adding special rims with different lengths and bending angles to obtain electronically switchable radiation patterns. Near field radiation of the array feeder is considered as the illuminator of the reflector antenna. The cosecant-squared pattern is arranged by determination of adequate near field distribution of the feeder. For this aim, waveguide feeder sources are excited with suitable phase and amplitude values to obtain the desired near field illumination.

The calculated near field distributions on the reflector for the pencil beam and cosecant-squared patterns are shown in Fig. 10 and Fig. 11. Feeder sources have same phases and amplitudes for pencil-beam. However, 7° phase differences are preferred and amplitude of the third source is increased 1.2 times for cosecant-squared pattern. H-plane normalized directivity gain patterns of the electronically switchable cosecant-squared and pencil-beam radiator are shown in Fig. 12.

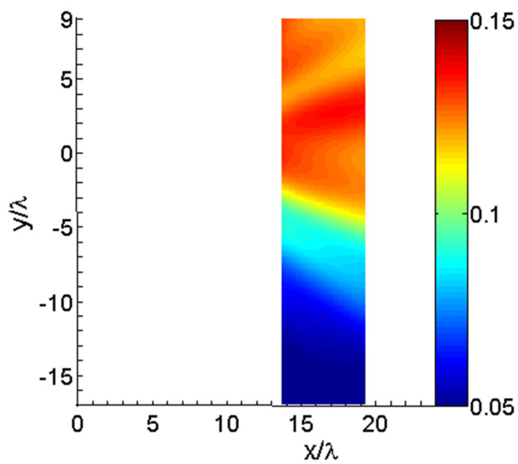

Fig. 10. Calculated near field which illuminates the reflector for pencil-beam radiation pattern.

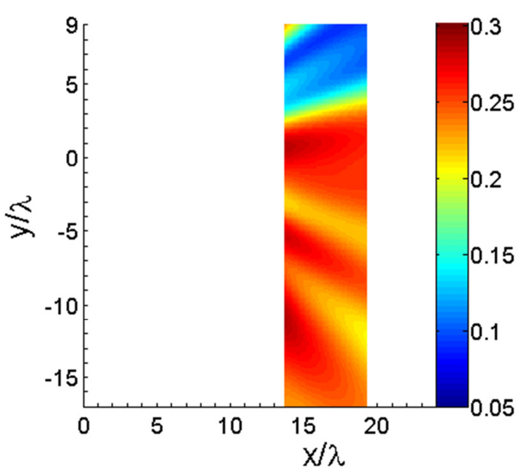

Fig. 11. Calculated near field which illuminates the reflector for cosecant-squared radiation pattern.

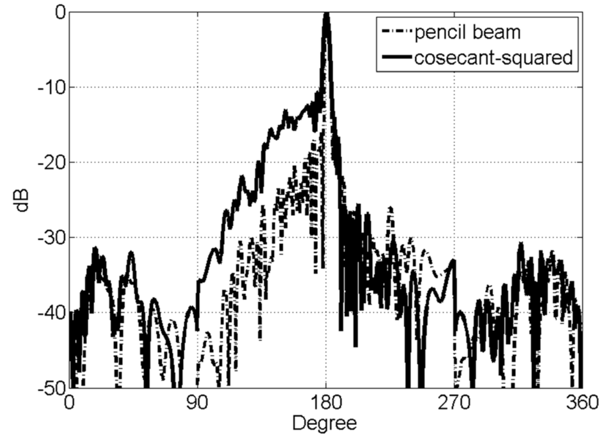

Fig. 12. H-plane normalized directivity gain patterns of the electronically switchable cosecant-squared and pencil-beam radiator.

Table 3: Segment lengths of the reflector contour regions

No	Segment Definition	Segment Length
1	$-\pi \le \theta < 2L_1 \dfrac{\pi}{L} - \pi$	$L_1 = 2b \tan\left(\left(\alpha_2 - \alpha_1\right)/2\right)$
2	$2L_1 \dfrac{\pi}{L} - \pi \le \theta < 2L_2 \dfrac{\pi}{L} - \pi$	$L_2 = L_1 + \pi c_2$
3	$2L_2 \dfrac{\pi}{L} - \pi \le \theta < 2L_3 \dfrac{\pi}{L} - \pi$	$L_3 = L_2 + 2a \tan\left(\left(\alpha_2 - \alpha_1\right)/2\right)$
4	$2L_3 \dfrac{\pi}{L} - \pi \le \theta < 2L_4 \dfrac{\pi}{L} - \pi$	$L_4 = L_3 + p_4 c_3$
5	$2L_4 \dfrac{\pi}{L} - \pi \le \theta < 2L_5 \dfrac{\pi}{L} - \pi$	$L_5 = L_4 + p_3 c_3$
6	$2L_5 \dfrac{\pi}{L} - \pi \le \theta < 2L_6 \dfrac{\pi}{L} - \pi$	$L_6 = L_5 + p_2 c_3$
7	$2L_6 \dfrac{\pi}{L} - \pi \le \theta < 2L_7 \dfrac{\pi}{L} - \pi$	$L_7 = L_6 + p_1 c_3$
8	$2L_7 \dfrac{\pi}{L} - \pi \le \theta < 2L_8 \dfrac{\pi}{L} - \pi$	$L_8 = L_7 + \pi c_2$
9	$2L_8 \dfrac{\pi}{L} - \pi \le \theta < 2L_9 \dfrac{\pi}{L} - \pi$	$L_9 = L_8 + + p_1 c_3$
10	$2L_9 \dfrac{\pi}{L} - \pi \le \theta < 2L_{10} \dfrac{\pi}{L} - \pi$	$L_{10} = L_9 + p_2 c_3$
11	$2L_{10} \dfrac{\pi}{L} - \pi \le \theta < 2L_{11} \dfrac{\pi}{L} - \pi$	$L_{11} = L_{10} + p_3 c_3$
12	$2L_{11} \dfrac{\pi}{L} - \pi \le \theta < \pi$	$L = L_{11} + p_4 c_3$
$c_1 = \left(b - a\right)/\left(1 + \cos\left(\alpha_3\right)\right)$ $c_2 = \left(b - a\right)/\left(1 + \cos\left(\alpha_2\right)\right)$		

Table 4: Parametric definitions of the reflector contour regions

No	Region	Parameterization
1	*AB*	$x=-2b\cos(\psi_1)/(1+\cos(\psi_1))$ $y=2b\sin(\psi_1)/(1+\cos(\psi_1))$
2	*BC*	$x=c_2\cos[(L_1-l)/c_2+\pi-\alpha_2]$ $-(a+b)\cos\alpha_2/(1+\cos\alpha_2)$ $y=c_2\sin[(L_1-l)/c_2+\pi-\alpha_2]$ $+(a+b)\sin\alpha_2/(1+\cos\alpha_2)$
3	*CD*	$x=-2a\cos(\psi_2)/(1+\cos(\psi_2))$ $y=2a\sin(\psi_2)/(1+\cos(\psi_2))$
4	*DE*	$x=-2a\cos(\alpha_1)/(1+\cos(\alpha_1))+(l-L_3)\cos(\alpha_3)$ $y=2a\sin(\alpha_1)/(1+\cos(\alpha_1))-(l-L_3)\sin(\alpha_3)$
5	*EF*	$x=-2a\cos(\alpha_1)/(1+\cos(\alpha_1))$ $+p_4c_3\cos(\alpha_3)+(l-L_4)\cos(\alpha_4)$ $y=2a\sin(\alpha_1)/(1+\cos(\alpha_1))$ $-p_4c_3\sin(\alpha_3)+(l-L_4)\sin(\alpha_4)$
6	*FG*	$x=-2a\cos(\alpha_1)/(1+\cos(\alpha_1))+(l-L_5)\cos(\alpha_5)$ $+c_3[p_4\cos(\alpha_3)+p_3\cos(\alpha_4)]$ $y=2a\sin(\alpha_1)/(1+\cos(\alpha_1))-(l-L_5)\sin(\alpha_5)$ $-c_3[p_4\sin(\alpha_3)+p_3\sin(\alpha_4)]$
7	*GH*	$x=-2a\cos(\alpha_1)/(1+\cos(\alpha_1))+(l-L_6)\cos(\alpha_6)$ $+c_3[p_4\cos(\alpha_3)+p_3\cos(\alpha_4)+p_2\cos(\alpha_5)]$ $y=2a\sin(\alpha_1)/(1+\cos(\alpha_1))-(l-L_6)\sin(\alpha_6)$ $-c_3[p_4\sin(\alpha_3)+p_3\sin(\alpha_4)+p_2\sin(\alpha_5)]$
8	*HI*	$x=c_1\cos[(L_7-l)/c_1-\alpha_1]-(a+b)\cos(\alpha_1)/(1+\cos(\alpha_1))$ $+c_3[p_4\cos(\alpha_3)+p_3\cos(\alpha_4)+p_2\cos(\alpha_5)+p_1\cos(\alpha_6)]$ $y=c_1\sin[(L_7-l)/c_1-\alpha_1]+(a+b)\sin(\alpha_1)/(1+\cos(\alpha_1))$ $-c_3[p_4\sin(\alpha_3)+p_3\sin(\alpha_4)+p_2\sin(\alpha_5)+p_1\sin(\alpha_6)]$
9	*IJ*	$x=c_1\cos(\pi+\alpha_1)-(a+b)\cos(\alpha_1)/(1+\cos(\alpha_1))-(l-L_8)\cos(\alpha_6)$ $+c_3[p_4\cos(\alpha_3)+p_3\cos(\alpha_4)+p_2\cos(\alpha_5)+p_1\cos(\alpha_6)]$ $x=c_1\sin[-\pi-\alpha_1]+(a+b)\sin(\alpha_1)/(1+\cos(\alpha_1))+(l-L_8)\sin(\alpha_6)$ $-c_3[p_4\sin(\alpha_3)+p_3\sin(\alpha_4)+p_2\sin(\alpha_5)+p_1\sin(\alpha_6)]$
10	*JK*	$x=c_1\cos(\pi+\alpha_1)-(a+b)\cos(\alpha_1)/(1+\cos(\alpha_1))-(l-L_9)\cos(\alpha_5)$ $+c_3[p_4\cos(\alpha_3)+p_3\cos(\alpha_4)+p_2\cos(\alpha_5)]$ $y=c_1\sin(-\pi-\alpha_1)+(a+b)\sin(\alpha_1)/(1+\cos(\alpha_1))+(l-L_9)\sin(\alpha_5)$ $-c_3[p_4\sin(\alpha_3)+p_3\sin(\alpha_4)+p_2\sin(\alpha_5)]$
11	*KL*	$x=c_1\cos(\pi+\alpha_1)-(a+b)\cos(\alpha_1)/(1+\cos(\alpha_1))$ $-(l-L_{10})\cos(\alpha_4)+c_3[p_4\cos(\alpha_3)+p_3\cos(\alpha_4)]$ $x=c_1\sin(-\pi-\alpha_1)+(a+b)\sin(\alpha_1)/(1+\cos(\alpha_1))$ $+(l-L_{10})\sin(\alpha_4)-c_3[p_4\sin(\alpha_3)+p_3\sin(\alpha_4)]$
12	*LM*	$x=c_1\cos(\pi+\alpha_1)-(a+b)\cos(\alpha_1)/(1+\cos(\alpha_1))$ $-(l-L_{11})\cos(\alpha_3)+c_3p_4\cos(\alpha_3)$ $x=c_1\sin(-\pi-\alpha_1)+(a+b)\sin(\alpha_1)/(1+\cos(\alpha_1))$ $+(l-L_{11})\sin(\alpha_3)-c_3p_4\sin(\alpha_3)$
$\psi_1=\alpha_1+[(\alpha_2-\alpha_1)/L_1]$, $\psi_2=\alpha_2-[(\alpha_2-\alpha_1)(l-L_2)/(L_3-L_2)]$		

V. CONCLUSION

In this work, the waveguide array fed parabolic reflector antenna is investigated to obtain electronically switchable pencil beam and cosecant-squared patterns. For this aim, the waveguide array structure is parametrically analyzed, and the modified asymmetric reflector geometry is proposed.

The Analytical Regularization Method is used to compute the near field distribution of the waveguide array feeder and the radiation patterns of the designed parabolic reflector antenna.

Simulation results of the feeder analysis and its combination with the modified reflector are presented to demonstrate the suitability of the proposed antenna for microwave and millimeter wave air, naval and coastal surveillance radars.

ACKNOWLEDMENT

This work was supported by grant PIRSES-GA-2010-269157 (AMISS project) of EU 7th Framework Marie Curie Actions research fund.

REFERENCES

[1] C. F. Winter, "Dual Vertical Beam Properties of Doubly Curved Reflectors", *IEEE Trans. Antennas Propagation*, vol. 19, no. 2, 1971.

[2] Y. Rahmat-Samii "A comparison between GO/Aperture field and physical optics methods for offset reflectors", *IEEE Trans. Antennas Propagation*, vol. Ap-32, no. 3, pp. 301-306, 1984.

[3] D. Duan, Y. Rahmat-Samii "A generalized diffraction synthesis technique for high performance reflector antennas", *IEEE Trans. Antennas Prop.*, vol. 43, no. 1, pp. 27-40, 1995.

[4] G. A. Suedan, E. V. Jull, "Beam Diffraction by Planar and Parabolic Reflectors", *IEEE Trans. Antennas Propagation*, vol. 39, pp. 521-527, 1991.

[5] K. Tap, P. H. Pathak, "A fast hybrid asymptotic and numerical physical optics analysis of very large scanning cylindrical reflectors with stacked linear array feeds", *IEEE Trans. Antennas Propagation*, vol. 54, no. 4, pp. 1142-1151, 2006.

[6] S. L. Avila, W. P. Carpes Jr, J. A. Vasconcelos, "Optimization of an offset reflector antenna using genetic algorithms", *IEEE Trans. Magnetics*, vol. 40, no. 2, pp. 1256-1259, 2004.

[7] F. Arndt, J. Brandt, V. Catina, J. Ritter, I. Rullhusen, J. Dauelsberg, U. Hilgefort, W. Wessel, "Fast CAD and optimization of waveguide components and aperture antennas by hybrid MM/FE/MoM/FD methods: State of the art

and recent advances”, *IEEE Trans. Mic. Theory Tech.*, vol. 52, no. 1, pp. 292-305, 2004.

[8] W. Ewe, L. Li, Q. Wu, M. Leong, “Analysis of reflector and horn antennas using adaptive integral methods*”, IEICE Trans. Comm.*, vol. E88-B, no. 6, pp. 2327-2333, 2005.

[9] M. Djordjevic, B. M. Notaros, “Higher order hybrid method of moments-physical optics modeling technique for radiation and scattering from large perfectly conducting surfaces”, *IEEE Trans. Antennas Prop.*, vol. 53, no. 2, pp. 800-813, 2005.

[10] A. S. Turk, “Analysis of aperture illumination and edge rolling effects for parabolic reflector antenna design”, *International Journal of Electronics and Comm. (AEUE)*, vol. 60, pp. 257-266, 2006.

[11] K. Umashankar, A. Taflove, *Computational Electromagnetics*, Artech House, 1993.

[12] J. H. Wilkinson, *The Algebraic Eigenvalue Problem*, Clarendon Press, Oxford, 1965.

[13] C. A. J. Fletcher, *Computational Galerkin Method*, Springer- Verlag, Berlin, 1984.

[14] Y. A. Tuchkin, “Wave scattering by an open cylindrical screen of arbitrary profile with Dirichlet boundary value condition”, *Soviet Physics Doclady*, vol. 30, pp. 1027-1030, 1985.

[15] Y. A. Tuchkin, E. Karacuha, A. S. Turk, “Analytical regularization method for E-polarized electromagnetic wave diffraction by arbitrary shaped cylindrical obstacles”, *7th Int. Conf. Math. Methods Electromagnetic Theory*, pp. 733-735, Kharkov, Sept. 1998.

[16] E. Karacuha, A. S. Turk, “E-polarized scalar wave diffraction by perfectly conductive arbitrary shaped cylindrical obstacles with finite thickness”, *Int. J. Infrared & Millimeter Waves*, vol. 22, pp. 1531-1546, 2001.

[17] M. Hashimoto, M. Idemen, O. A. Tretyakov, "*Analytical and Numerical Methods in Electromagnetic Wave Theory*", Science House Co., p. 202, 1992.

[18] A. S. Turk, O. Yurduseven, “Parametric analysis of multi-source feeding flare rolling and corrugating effects for H-plane horn radiator”, *Applied Comp. Electromagnetic Society (ACES) Journal*, vol. 25, no. 11, pp. 990-997, 2010.

[19] A. S. Turk, O. Yurduseven, "Parametric design of parabolic reflector antenna with switchable cosecant-squared pattern", *Applied Comp. Electromagnetic Society (ACES) Journal*, Issue 6, vol. 26, pp. 494-501, 2011.

[20] A. S. Turk, O. M. Yucedag, "Parametric analysis of flare edge rolling throat bending and asymmetric flare effects for H-plane horn radiator", *International Journal of Electronics and Communication (AEUE)*, Issue 4, vol. 66, pp. 297-304, 2012.

Okan Mert Yucedag received the B.S. and M.S. degrees in Electronics Engineering from Uludag University, Bursa-Turkey in 2006 and 2009, respectively. He joined the Scientific and Technical Research Council of Turkey (TUBITAK) in 2007. He is currently working as senior researcher at TUBITAK Information Technologies Institute.

His research interests are microwave radar systems, antenna design, RCS estimation and numerical methods in electromagnetic wave scattering, especially method of moments and analytical regularization method.

Ahmet Serdar Turk received the B.S. degree in Electronics-Communication Engineering from Yildiz Technical University, Istanbul, Turkey in 1996. He received M.S. and Ph.D. degrees in Electronics Engineering from Gebze Institute of Technology, in 1998 and 2001, respectively. He joined the Scientific and Technical Research Council of Turkey (TUBITAK) in 1998. He is currently working as professor at Yildiz Technical University Electronics Engineering Department.

His research interests include horn, reflector, array and ultra-wide band antenna designs in RF and microwave bands, numerical methods in electromagnetic wave scattering, high frequency surface wave radar, ground penetrating radar, and microwave and millimeter wave radar systems.